Optimization of Tunnel Blasting and Support Parameters Using the HJC Numerical Model: A Fluid-Solid Coupling Approach

Wenting Dai*[iD], Kunpeng Fang[iD]

Collage of Construction, Jilin University, 130026 Changchun, China

* Correspondence: Wenting Dai (daiwt@jlu.edu.cn)

Abstract: The optimization of tunnel blasting parameters and support designs is critical for enhancing both structural stability and engineering efficiency. This study employs the Holmquist-Johnson-Cook (HJC) numerical model to simulate the blasting process of the Xiahong Tunnel in China, with a particular focus on the vibration velocity and damage zones at various locations. A fluid-solid coupling method is applied to model the interaction between the surrounding rock and blasting forces, and the effects of different detonation sequences and radial uncoupling coefficients on the peak vibration velocities and damage domains are thoroughly examined. The results indicate that blasting from the outside to the inside results in a more cohesive damage domain compared to the traditional inside-out approach. Specifically, the peak vibration velocity of the surrounding rock during inside-out blasting reaches 161.4 cm/s, which is higher than the 82.2 cm/s observed with outside-in blasting. Therefore, the outside-in blasting sequence is identified as the more optimal strategy. Furthermore, an increase in the radial decoupling coefficient gradually reduces the damage domain, with the coefficient k = 2.0 showing no significant improvement in damage domain reduction. However, a decoupling coefficient that is too small leads to excessive over-excavation. Based on this analysis, the optimal radial decoupling coefficient is found to be k = 1.5, offering the most balanced damage domain reduction without causing over-excavation. The analysis also explores the influence of the initial lining thickness of sprayed concrete on the vibration characteristics of the surrounding rock. Both structural stability and economic considerations suggest an ideal thickness for the initial lining. The findings of this study provide valuable guidance for the subsequent implementation of tunnel blasting and support optimization in engineering practices.

Keywords: Tunnel blasting; Fluid-solid coupling; Numerical simulation; Radial decoupling coefficient; Damage domain; Vibration velocity; Initial lining thickness; Blasting sequence

1 Introduction

With the continuous growth of the global economy and advancements in technology, tunnel excavation projects have seen a marked increase. The drilling and blasting processes involved in tunnel construction are subject to various influencing factors, including terrain conditions, environmental factors, and rock types. As such, the use of numerical simulation to investigate the various parameters associated with the blasting process has become increasingly critical.

Among the key parameters influencing tunnel excavation, blasting and support parameters are of particular significance [1–4]. These parameters are typically determined through on-site measurements, empirical judgment, or data simulation [5–10]. However, on-site measurements entail high costs and risks, and empirical methods often lack the precision required for accurate parameter estimation. In contrast, numerical simulation, which offers advantages in terms of accuracy, predictability, safety, efficiency, and cost-effectiveness, has emerged as the most widely adopted method for determining blasting and excavation parameters [11–14]. Over the past few decades, rapid advancements in computer technology have facilitated the integration of numerical simulation into various fields [15–17]. In tunnel blasting, numerical simulation can be employed to model the surrounding rock damage and vibration velocities at the excavation surface, among other factors [18–21]. The resulting data allow for more accurate and scientifically grounded determinations of blasting parameters, providing a robust basis for real-world construction practices [22–25].

In this study, the ANSYS/LSDYNA finite element software is utilized to establish the HJC model, employing a fluid-solid coupling approach to analyze and optimize the blasting and support parameters for the blasting process of the Xiahong Tunnel section of the Cangtai Expressway. The findings from this analysis will offer valuable technical insights and serve as a reference for similar future projects.

2 Project Overview

The Xiahong Tunnel is located in Taishun County, Wenzhou City, Zhejiang Province, and serves as a key component of the Cangnan-Taishun Expressway. The tunnel has a total length of 1,717 meters, with the pile numbers ranging from LK0 + 390 to LK2 + 107. The tunnel's clear height is 5 meters, its clear width is 12 meters, and the maximum burial depth is 11 meters. To the east of the tunnel, within a 300-meter radius, the surrounding area consists of mountains, forests, open fields, and farmlands. The tunnel is located 300 meters south of Provincial Highway 331 and 254 meters from the nearest residential building in Xinyuan District. It is also connected to the Da'an Interchange Road. To the west and north, the surrounding terrain is characterized by mountains, forests, open fields, and farmlands. The 300-meter range surrounding the tunnel is primarily mountain forest land, open space, and farmland. The nearest private residence to the north is located 193 meters from the tunnel. Figure 1 presents an aerial view of the area surrounding the Xiahong Tunnel.

Figure 1. Aerial photo of Xiahong Tunnel

3 Establishment of Model

3.1 Determination of Simulation Method

For this numerical simulation, the surrounding rock is classified as grade III, primarily composed of interbedded rhyolite tuff and sandstone conglomerate. To simplify the calculation, rhyolite tuff was selected as the material for the simulation. The full-section blasting method is employed, using a segmental excavation approach, with each excavation cycle spanning 2.4 meters. The simulation adopts the fluid-solid coupling method, which accurately models the interaction between the fluid (explosive gases) and the solid medium (surrounding rock) during the explosion. This interaction is essential for understanding the propagation of the explosion shock wave, the distribution of energy, and the damage mechanism within the medium. By accounting for the dynamic coupling between the fluid and solid phases, the fluid-solid coupling method provides a more realistic representation of the physical phenomena occurring during the explosion process. In contrast to traditional numerical simulation methods, where fluids and solids are typically treated as separate entities, often neglecting their interaction, the fluid-solid coupling approach integrates the two phases. This integrated approach leads to more accurate predictions of the extent and distribution of damage caused by the explosion, enhancing both the precision and reliability of the simulation results.

3.2 Material Parameters of the Model

The HJC model and the Riedel-Hiermaier-Thoma (RHT) model are widely used in the numerical simulation of tunnel blasting. Compared to the RHT model, the HJC model offers a broader capability to simulate the behavior of soil under various dynamic loads, including blast impacts, hammer impacts, and seismic forces. Due to its versatility and adaptability across different engineering fields, the HJC model was selected for this numerical simulation.

The model incorporates several materials, including peripheral rock, air, emulsion explosives, and plugging soil. The fluid-solid coupling algorithm is employed throughout the simulation. Specifically, the rock phase is modeled using the Lagrange algorithm, while the fluid phase is simulated using the Arbitrary Lagrangian-Eulerian (ALE)

method. The chosen element type for the model is 3D_SOLID_164, which is suitable for the representation of solid and fluid interactions in the simulation.

The coupling of the HJC model with the ALE algorithm is implemented using the following steps:

(1) Geometric Model and Meshing: A geometric model is created, including the geometries for explosives, air domains, and rock structures. Lagrangian meshes are applied to the rock structures, with the HJC model parameters assigned to these elements. The interaction between the Eulerian grids for explosives and air is facilitated through the fluid-structure coupling algorithm.

(2) Material Model and Equation of State: The material model and the corresponding equation of state are defined to characterize the behavior of the involved materials.

(3) Fluid-Structure Coupling: The fluid-structure coupling is defined to model the interaction between the explosive fluids and the surrounding rock structures.

(4) ALE Control and Grid Redraw Parameters: ALE control settings and grid redrawing parameters are established to ensure accurate tracking of material motion and deformation during the simulation.

(5) Solution and Post-Processing: The model is solved, and post-processing is performed to analyze the results of the simulation.

The primary rock type in the area surrounding the Xiahong Tunnel is rhyolitic tuff. The material parameters for its HJC intrinsic model are provided in Table 1.

Table 1. Parameters of the HJC constitutive model for tuff

ρ_0 / kg·m^{-3}	G / MPa	f_c / MPa	A	B	C	N	S$_{max}$	D$_1$	D$_2$
1680	6543	50	0.55	1.77	0.0097	0.77	17	0.04	1

T / MPa	p_c / MPa	μ_c	p_i / MPa	μ_1	K$_1$ / GPa	K$_2$ / GPa	K$_3$ / GPa	ε_0 / s^{-1}	ε_f / min
3.3	17	0.00253	2500	0.38	3.1	6	8.4	5E - 5	0.01

Note: ρ_0 is the density of tuff; G is the shear modulus of the rock; f_c is the quasi-static uniaxial compressive strength; A is the characteristic viscous strength coefficient; B is the pressure-hardening coefficient; C is the strain-rate-influenced parameter; N is the pressure-hardening exponent; Smax is the maximum characteristic equivalent stress of the material; D$_1$ and D$_2$ are the damage-related variables; T is the maximum tensile hydrostatic pressure; p_c is the crushing pressure of the rock; p_l is the locking pressure; μ_c, μ_l are the volume strain coefficients; K$_1$, K$_2$, K$_3$ are the pressure constants; ε_0 is the reference strain rate; ε_f is the plastic strain before fracture

The explosive used for blasting is emulsified explosive, and the material is 008 HIGH_EXPLOSIVE_BURN. The material parameters are shown in Table 2.

Table 2. Material parameters of emulsion explosive

ρ_0 / kg· m^{-3}	Detonation Velocity / m·s^{-1}	Pressure on the Detonation Wavefront / GPa
1630	6930	27

The borehole structure consists of an inner charge of emulsion explosive and an outer soil plug. Therefore, it is necessary to establish a constitutive model for the plugging soil. The soil plug is modeled using the *MAT_SOIL_AND_FOAM* material model (*MAT 005*), and its main parameters are listed in Table 3.

Table 3. Partial material parameters of the soil plug

ρ_0 / kg· m^{-3}	G / MPa	Bulk / GPa	A$_0$	A$_1$	A$_2$	P$_c$	E$_2$	E$_3$	E$_4$
1800	6385	30	3.4E - 4	703.3	3E + 9	-69	-0.104	-1.61	-1.92

Note: G is the shear modulus of soil; bulk is the bulk modulus during unloading. A$_0$, A$_1$, and A$_2$ are yield function constants. P_c is the cut-off value of tensile pressure; E$_2$, E$_3$, and E$_4$ are the volumetric strain values.

3.3 Model Construction

The dimensions of the tunnel and the arrangement of blast holes used during excavation are shown in Figure 2. According to Saint-Venant's principle, the overall model size must be at least twice that of the tunnel excavation. Therefore, the surrounding rock mass is modeled with dimensions of 36 m × 24 m × 5 m, as illustrated in Figure 3. The fluid domain covers the entire excavation area. A model with a blast-hole depth of 1.5 m and a stemming depth of 0.5 m is constructed, as shown in Figure 4, where the charge radius is 2.5 cm. The air domain model is presented

in Figure 5. The equation of state for the explosive adopts the JWL equation, and its specific form is given in Eq. (1).

$$P_1 = A\left(1 - \frac{\omega}{R_1 V}\right)e^{-R_1 V} + B\left(1 - \frac{\omega}{R_2 V}\right)e^{-R_2 V} + \frac{\omega E s}{V}$$

(1)

In the formula, A, B, R_1, R_2, ω are the coefficients of the equation of state, GPa; E_1 is specific internal energy, GPa; V_0 is the relative volume of detonation product. The specific parameters can be seen in Table 4.
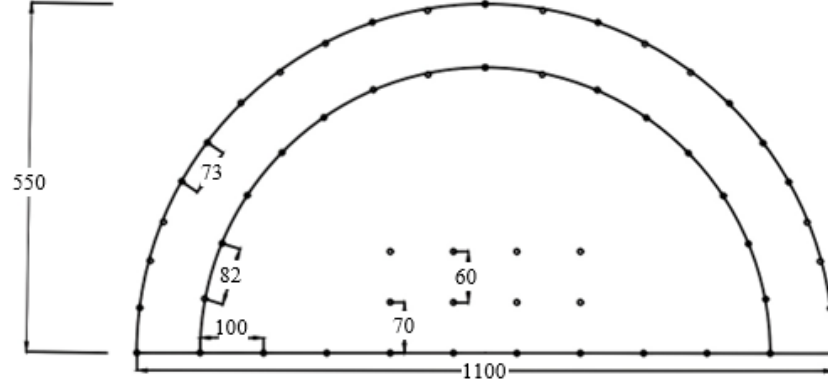

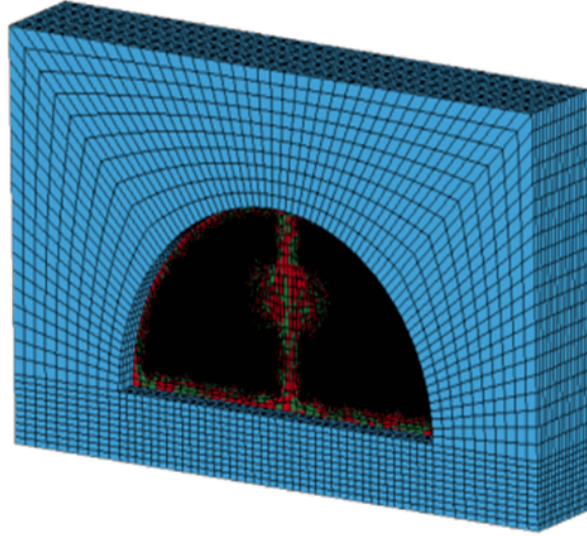**Figure 2.** Schematic diagram of tunnel dimensions and boreholes
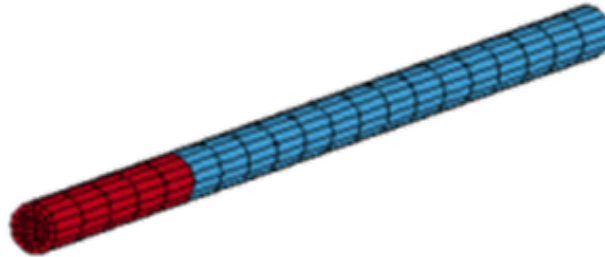

Figure 3. Tunnel model

Figure 4. Blockage and explosive model
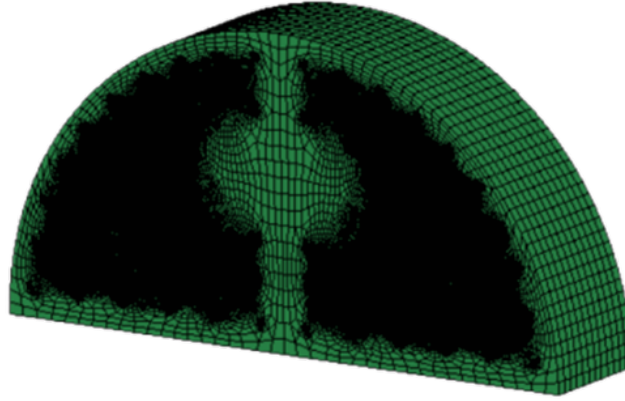
Figure 5. Fluid domain model

Table 4. Parameters of JWL equation for explosives

A / GPa	B / GPa	R_1	R_2	ω	E / GPa	V
371	7.23	4.15	0.95	0.3	7.0	1.0

The equation of state of the air in the model is LINEAR_POLYNOMIAL, and the specific equation expression can be seen in Eq. (2).

$$p = C_0 + C_1\mu + C_2\mu^2 + C_3\mu^3 + \left(C_4 + C_5\mu + C_6\mu^2\right) E \tag{2}$$

In the formula, C_0, C_1, C_2, C_3, C_4, C_5 and C_6 are coefficient constants of the polynomial equation. Since the fluid domain in this simulation is air, $C_0 = C_1 = C_2 = C_3 = C_6 = 0$, $C_4 = C_5 = 0.4$. E is the unit of initial internal energy, GPa. μ is the constant in the equation, and its calculation formula can be seen in Eq. (3).

$$\mu = \frac{1}{V} - 1 \tag{3}$$

In the formula, V is the initial relative volume.
Set the detonation interval between the boreholes to 100 μs and the total detonation time to 1000 μs.
In summary, the various parameter indicators of this model can be seen in Table 5.

Table 5. Parameters of tunnel model

Tunnel Burial Depth / m	Vertical Geostress / MPa	Blasting Parameters				
		Single hole charge quantity / kg	Number of holes	Time interval / μs	Borehole depth / m	Depth of blockage / m
11	0.28	3.3	56	1000	1.5	0.5

4 Optimization Analysis of Blasting Plan

4.1 Influencing Factors of Blasting Effect

In this simulation, the damage domain and vibration velocity are selected as the primary analysis results.

The damage domain describes the extent and degree of material or structural damage caused by the blasting action. In numerical simulations, the damage domain is typically determined by analyzing changes in stress, strain, energy, and other physical quantities during the blasting process. These variations reflect the material damage and failure resulting from the blast. Consequently, the damage domain serves as an effective metric for evaluating whether the blasting operation meets the intended objectives in tunnel excavation.

Vibration velocity represents the propagation velocity of the vibration waves generated by the blasting process within the medium. The vibration waves, induced by the energy released during blasting, propagate through the surrounding rock, causing vibration effects on nearby objects and structures. Given the proximity of residential buildings and other civilian facilities, located 254 m from the Xiahong Tunnel, the impact of vibration velocity on

these structures must be considered during the blasting process. In the simulation, the vibration velocity is calculated by analyzing the propagation characteristics of the vibration waves. The magnitude and distribution of the vibration velocity indicate the strength and extent of the blast's impact on the surrounding environment. By selecting vibration velocity as a key reference, the simulation can assess whether the impact on nearby structures meets the relevant safety and regulatory standards.

4.2 Blast Mechanical Response Parameters

In this numerical simulation, the blasting parameters—namely the detonation sequence and the radial decoupling coefficient—must be determined, as both parameters play a critical role in tunnel blasting and excavation. The detonation sequence is essential for controlling the propagation direction and energy distribution of the blast waves. A well designed detonation sequence can effectively regulate the blasting energy release, thereby improving contour control and reducing overbreak and underbreak. Optimizing the sequence contributes to maintaining tunnel profile smoothness and excavation quality while also reducing blast induced vibrations and safeguarding the stability of surrounding structures. The radial decoupling coefficient, defined as the ratio of borehole diameter to charge diameter, is another key factor influencing blasting performance. A reasonable decoupling coefficient helps control the transmission and distribution of explosive energy, achieving a more uniform and effective blasting result. An excessively large coefficient may cause insufficient energy transfer to the surrounding rock, leading to underbreak, whereas an overly small coefficient may concentrate energy excessively, resulting in overbreak and damage to the perimeter rock mass. Accurate control of the radial decoupling coefficient is therefore crucial for achieving the desired excavation effect. In summary, both detonation sequence and radial decoupling coefficient are indispensable blasting parameters in tunnel excavation. Their optimization enables more precise, efficient, and safer blasting operations, ensuring the smooth progress of the tunnel project. With ongoing advances in blasting technology and research, the importance of these parameters and their optimization methods continues to grow.

4.3 Blast Mechanical Response Analysis

Three different blasting scenarios are analyzed in this simulation: (1) Blasting Program 1 (Normal Detonation); (2) Blasting Program 2 (Modified Detonation Sequence); (3) Blasting Program 3 (Adjusted Radial Decoupling Coefficient).

In Blasting Program 1, the detonation sequence follows the standard approach: initial detonation of the hollowing holes, followed by detonation of the auxiliary holes, and then the peripheral holes at the bottom. The detonation interval is set to 100 μs, and the radial uncoupling coefficient is fixed at k = 1.5. Simulation results for detonation intervals of 200 μs and 600 μs are presented in the explosion damage cloud diagrams shown in Figure 6.

(a) (b)

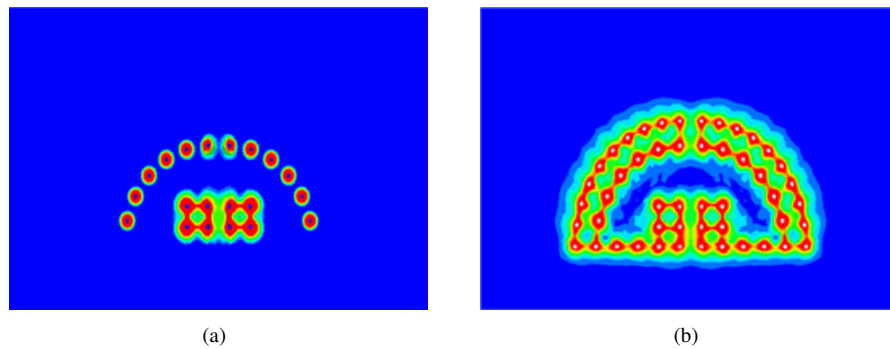**Figure 6.** Damage cloud image under normal initiation: (a) 200 μs damage cloud image; (b) 600 μs damage cloud image

As shown in the figure, during the initial blasting, the damage domain of a single borehole extends radially outward from the detonation point, forming a circular damage region. As the blasting progresses, the damage areas from multiple boreholes merge, creating an overall damage zone. It has been established that tunnel blasting typically results in the formation of a crushed zone and a fissure zone around each borehole. The radius of the crushed zone is typically 2 to 3 times the radius of the borehole charge, while the radius of the fissure zone is generally 12 to 15 times the charge radius. In this simulation, the charge radius is set to 2.5 cm. The measured radius of the crushed zone ranges from 6 to 7 cm, and the radius of the fissure zone is between 30 and 35 cm, which is consistent with the results reported in previous studies.

Blasting Program 2 uses the following detonation sequence: the bottom hole and peripheral holes are detonated first, followed by detonation of the auxiliary and trenching holes. The radial uncoupling coefficient is set to k = 1.5.

Damage cloud diagrams at 200 μs and 600 μs intervals are shown in Figure 7. The radius of the crushed zone is between 10 and 11 cm, while the radius of the fissure zone ranges from 50 to 55 cm, as shown in Figure 7. These results illustrate the damage distribution at the specified time intervals. The corresponding damage cloud diagrams for 200 μs and 600 μs can be found in Figure 8. The peak vibration velocity, as a result of the combined detonation sequence, is provided in Table 6.

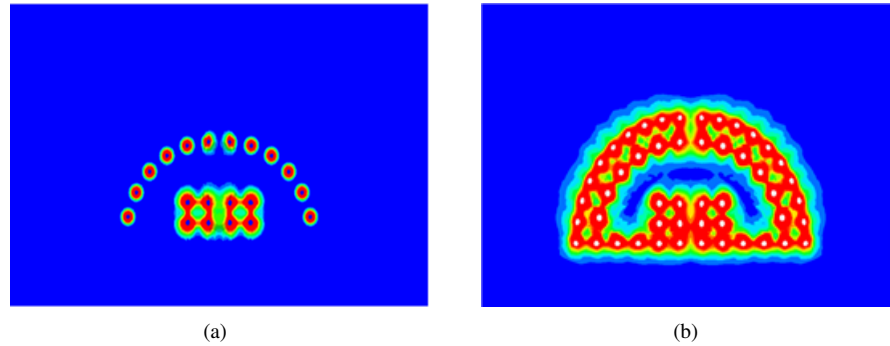(a)   (b)

Figure 7. Damage cloud image of detonation after changing the sequence: (a) 200 μs damage cloud image; (b) 600 μs damage cloud image

(a) The point closing velocity under normal initiation   (b) The combination velocity of each point after changing the sequence of detonation
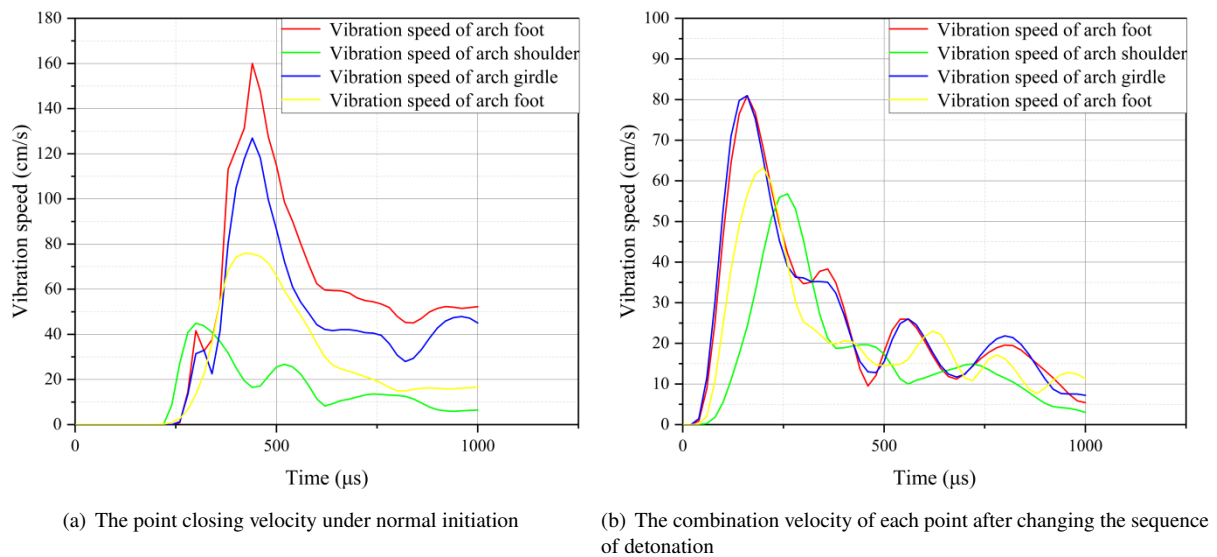
Figure 8. The combination velocity of each point in blasting

Table 6. Peak vibration velocity before and after changing blasting sequence at different positions

Surrounding Rock Position	Peak Value of Initial Vibration Velocity / cm·s⁻¹	Peak Vibration Velocity after Changing the Sequence / cm·s⁻¹
Arch springing	161.4	82.2
Arch shoulder	127.6	81.3
Arch springing line	77.6	64.5
Arch crown	42.2	56.6

Blasting Program 3 follows the same detonation sequence as Blasting Program 1, but with adjustments to the radial decoupling coefficient. The radial decoupling coefficient, defined as the ratio of the borehole diameter to the diameter of the explosive charge, has a significant impact on the blasting-induced damage to the surrounding rock. It has been observed that varying the decoupling coefficient can help alleviate over-excavation damage to the surrounding rock, while also offering cost-saving benefits. In this simulation, damage maps for decoupling coefficients of k = 1.25, k = 1.5, k = 1.75, and k = 2.0 are shown in Figure 9.
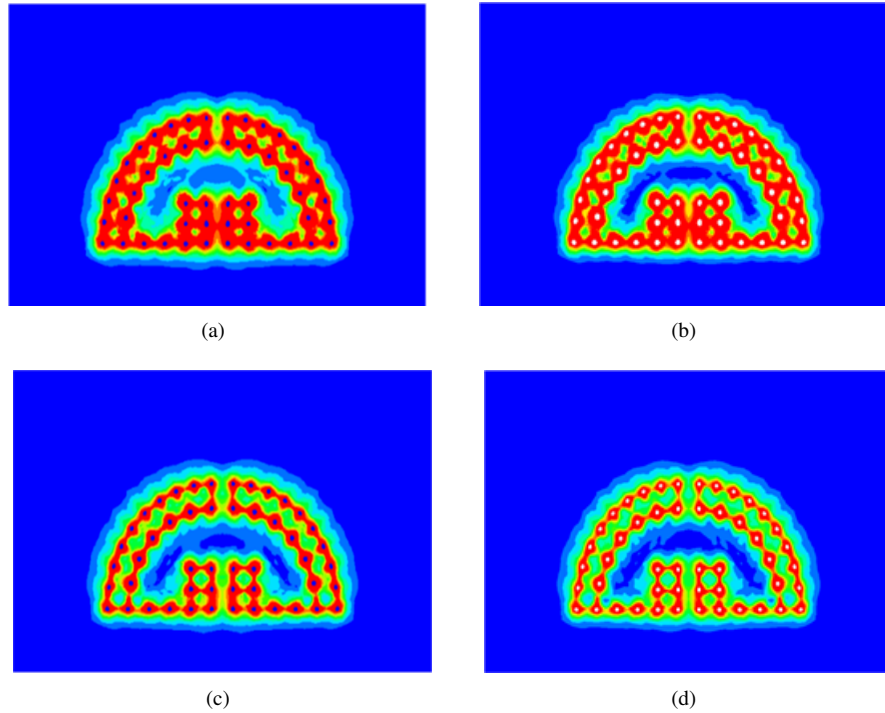
Figure 9. Cloud image of blasting damage under different radial uncoupling coefficients: (a) Damage cloud image with k = 1.25; (b) Damage cloud image with k = 1.5; (c) Damage cloud image with k = 1.75; (d) Damage cloud image with k = 2.0

4.4 Optimization Results of the Blasting Program

By comparing and analyzing the damage cloud maps and vibration velocities of Blasting Program 1 and Blasting Program 2, it can be observed that, after altering the blasting sequence, the damage domain caused by Blasting Program 2 is 66.7% larger than that of Blasting Program 1 at the same time intervals. Furthermore, the vibration velocities of Blasting Program 2 are 34.1% to 96.4% lower than those of Blasting Program 1. Due to the adverse impact of excessive vibration velocity on surrounding buildings, the plan of detonating the peripheral holes and bottom holes first is found to be more effective than detonating the cutting and auxiliary holes first.

An analysis of the damage maps of Blasting Program 2 and Blasting Program 3 reveals that, with an increase in the radial decoupling coefficient, the damaged area of the excavation gradually decreases. At a decoupling coefficient of k = 2.0, no coherent overall damage domain is formed, and compared to k = 1.5, the damage domain is reduced by approximately 59%. This reduction does not meet the requirements of the blasting process. As the decoupling coefficient decreases, the damage area gradually expands. When k = 1.25, the over-excavation caused by blasting is about 32% higher than that caused by k = 1.5. Over-excavation leads to a range of hazards, including safety risks, increased costs, construction difficulties, and impacts on groundwater, among others. To minimize these risks, over-excavation damage must be avoided as much as possible during tunneling. Therefore, a radial decoupling coefficient of k = 1.5 is deemed optimal. With k = 1.5, the tunnel forms a continuous damage domain, and the over-excavation damage remains within the allowable normative range.

Based on these results, the final blasting sequence is selected to begin with the detonation of the peripheral perimeter holes and bottom holes, followed by detonation of the center, hollowing holes, and auxiliary holes. The optimal radial decoupling coefficient is determined to be k = 1.5.

5 Determination of Supporting Parameters

5.1 Selection of Supporting Parameters

The thickness of shotcrete plays a crucial role as a supporting parameter in tunnel excavation blasting. Firstly, the thickness of shotcrete directly influences the strength and stability of the supporting structure. After tunnel blasting excavation, the surface of the rock or structure requires timely and effective support to prevent surrounding rock loosening, collapse, and other accidents. As a vital component of the support structure, the thickness of shotcrete significantly affects the overall support performance. An optimal shotcrete thickness can enhance the bearing capacity of the support structure and ensure the safety of tunnel construction. Secondly, shotcrete thickness is a key

factor in controlling the deformation of the surrounding rock. During tunnel blasting excavation, the surrounding rock is disturbed and damaged to varying degrees, resulting in deformation. The thickness of the shotcrete should be adjusted based on the extent of this deformation to control the movement of the surrounding rock. If the shotcrete is too thin, it may fail to adequately constrain the deformation of the surrounding rock. Conversely, excessive thickness can lead to material wastage and increased construction costs. Therefore, selecting the appropriate shotcrete thickness is critical to ensuring both the quality and safety of the tunnel construction process. Moreover, shotcrete thickness affects the overall stability and service life of the tunnel. As a critical piece of transportation infrastructure, the tunnel's stability and service life are directly linked to public safety and the economic and social development of the region. Adequate shotcrete thickness improves the overall stability of the tunnel, reducing the likelihood of safety accidents and minimizing maintenance costs associated with inadequate support. Consequently, in this simulation, the shotcrete thickness is considered as the primary supporting parameter.

5.2 Determine Supporting Parameters

The reference parameter used for determining the support parameters is the vibration velocity of the surrounding rock during blasting, with the established support model depicted in Figure 10. The shotcrete is made of C20 concrete, while the tunnel lining is constructed from C25 concrete. The specific material parameters are provided in Table 7. Blasting tests are conducted with shotcrete thicknesses set to 15 cm and 20 cm, respectively. The vibration velocities at various points on the excavation surface, including the vault, spinner, waist, and bottom of the arch, are recorded and presented in Figure 11.

By comparing the vibration velocities of the two blasting scenarios, it can be observed that the peak vibration velocity for the shotcrete with a thickness of 15 cm is 82.7 cm/s, with a corresponding deformation of the surrounding rock of 24 mm. In contrast, for shotcrete with a thickness of 20 cm, the peak vibration velocity is 78.6 cm/s, and the deformation of the surrounding rock is 19 mm. Both values comply with the code requirements for vibration velocity in tunnel blasting. However, excessively thick shotcrete can lead to an increase in internal voids, reducing the structural strength of the concrete. Moreover, heavy shotcrete can cause the material to crack and flake, compromising its integrity. Additionally, a thicker shotcrete layer requires more material, which not only increases construction costs but can also lead to unnecessary resource waste. Therefore, a shotcrete thickness of 15 cm is deemed optimal for balancing performance and cost-efficiency.
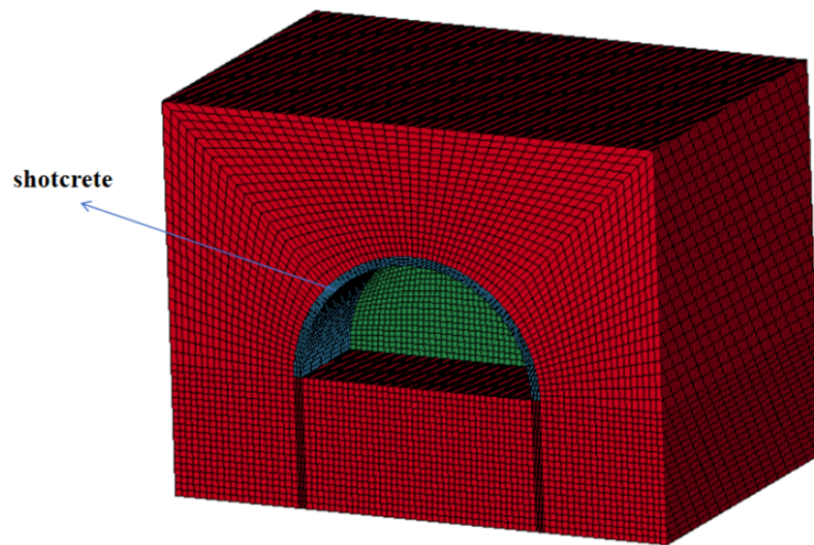

Figure 10. Shotcrete model

Table 7. Calculation parameters of primary lining and lining

Materials	Density ρ_0 / kg· m^{-3}	Modulus of Elasticity E / GPa	Poisson's Ratio
C20 concrete	2360	26	0.22
C25 concrete	2400	29	0.18

(a) Vibration velocity of 15cm thick concrete　　　(b) Vibration velocity of 20cm thick concrete
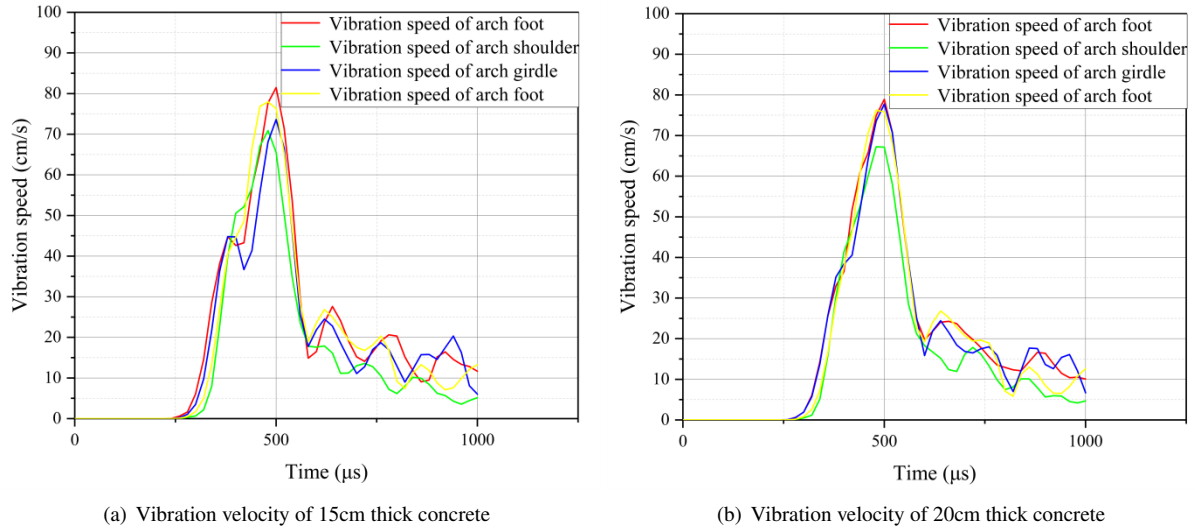
Figure 11. Vibration velocity after blasting shotcrete

6 Conclusions

In this study, the fluid-structure coupling method was employed to integrate the tunnel surrounding rock model with the fluid domain model, facilitating the simulation of the damage and vibration of surrounding rock during the tunnel blasting process. The primary objective was to determine the appropriate blasting and supporting parameters for tunnel excavation, and the following conclusions were drawn:

(1) Blasting and Supporting Parameters: The blasting and supporting parameters in tunnel excavation are influenced by multiple factors. Specifically, the blasting parameters are closely associated with the detonation sequence and the radial uncoupling coefficient, while the supporting parameters are predominantly determined by the thickness of shotcrete. Consequently, particular attention should be given to these parameters in practical engineering applications.

(2) Detonation Sequence: The results indicate that the detonation sequence has a significant impact on the damage domain and vibration velocity. When the detonation of the bottom hole and surrounding holes precedes that of the auxiliary holes, the damage domain is approximately 66.7% larger than when the traditional detonation sequence (excavation and auxiliary holes first) is used. Moreover, the vibration velocity in this sequence was found to be reduced by 34.1% to 96.4%, thereby minimizing the damage to surrounding buildings and infrastructure.

(3) Radial Uncoupling Coefficient: The radial uncoupling coefficient plays a crucial role in controlling the damage caused by blasting. The simulation results revealed that when the decoupling coefficient was set to k = 1.25, the over-excavation damage was approximately 32% higher than when k = 1.5. On the other hand, at k = 2.0, the damage domain decreased by 59% compared to k = 1.5, to the point where a coherent damage domain could no longer be formed. Based on these findings, a radial uncoupling coefficient of k = 1.5was selected as the optimal value for this simulation.

(4) Shotcrete Thickness: The thickness of shotcrete is a critical parameter affecting the stability of tunnel excavation. This study analyzed the vibration velocities of surrounding rock with shotcrete thicknesses of 15 cm and 20 cm. The results showed that the peak vibration velocity was 82.7 cm/s for a shotcrete thickness of 15 cm, with a corresponding surrounding rock deformation of 24 mm. In contrast, for 20 cm thickness, the peak vibration velocity was 78.6 cm/s, and the deformation was reduced to 19 mm. Both thicknesses complied with the specifications for allowable vibration velocity. However, excessively thick shotcrete leads to a reduction in concrete strength, potential detachment of the material, and unnecessary resource waste. Therefore, a shotcrete thickness of 15 cm is recommended for optimal performance.

Data Availability

The data used to support the findings of this study are available from the corresponding author upon request.

Conflicts of Interest

The authors declare that they have no conflicts of interest.

References

[1] H. B. Zhao, Y. Long, X. H. Li, and L. Lu, "Experimental and numerical investigation of the effect of blast-induced vibration from adjacent tunnel on existing tunnel," *KSCE J. Civ. Eng.*, vol. 20, no. 1, pp. 431–439, 2016. https://doi.org/10.1007/s12205-015-0130-9

[2] B. Zhang, C. Li, J. L. Li, R. Z. He, X. F. Zhang, X. G. Li, Z. J. Wang, and Y. Wu, "Experimental study on dynamic response of existing tunnel lining structure by adjacent tunnel blasting load," *Sci. Rep.*, vol. 15, no. 1, p. 28473, 2025. https://doi.org/10.1038/s41598-025-12687-z

[3] X. T. Zhao, Y. Liu, and X. D. Zhu, "Numerical simulation of blasting excavation across a soil-rock interface of highway tunnel," in *The 2nd ISRM International Young Scholars' Symposium on Rock Mechanics*, 2011, pp. 851–854.

[4] N. N. Minh, P. Cao, and Z. Z. Liu, "Contour blasting parameters by using a tunnel blast design mode," *J. Cent. South Univ.*, vol. 28, no. 1, pp. 100–111, 2021. https://doi.org/10.1007/s11771-021-4589-x

[5] Q. G. Liang, J. Li, D. W. Li, and E. F. Ou, "Effect of blast-induced vibration from new railway tunnel on existing adjacent railway tunnel in Xinjiang, China," *Rock Mech. Rock Eng.*, vol. 46, no. 1, pp. 19–39, 2012. https://doi.org/10.1007/s00603-012-0259-5

[6] L. H. Ma, F. Lin, Y. Q. Du, S. Ren, N. Z. Long, and P. Zhang, "Blasting profile evaluation of sand-mud interbedded surrounding rock during the large-span tunnel construction," *Sci. Rep.*, vol. 14, no. 1, p. 12405, 2024. https://doi.org/10.1038/s41598-024-62921-3

[7] H. Peng, S. L. Liu, and J. J. Yao, "Natural diffusion model of blasting fume in tunnel construction," in *International Conference on Computer Science, Environment, Ecoinformatics, and Education*, 2011, pp. 143–149. https://doi.org/10.1007/978-3-642-23345-6_28

[8] Q. B. Zhang, Z. X. Zhang, C. S. Wu, J. S. Yang, and Z. Y. Wang, "Characteristics of vibration waves measured in concrete lining of excavated tunnel during blasting in adjacent tunnel," *Coatings*, vol. 12, no. 7, p. 954, 2022. https://doi.org/10.3390/coatings12070954

[9] X. G. Jin, Q. Yan, Y. X. Zhang, and W. Liu, "Test on blasting vibration of neighborhood tunnel and discussion of safety vibration velocity," in *Progress in Safety Science and Technology*, 2020, pp. 787–793.

[10] N. Jiang and C. B. Zhou, "Blasting vibration safety criterion for a tunnel liner structure," *Tunn. Undergr. Space Technol.*, vol. 32, pp. 52–57, 2012. https://doi.org/10.1016/j.tust.2012.04.016

[11] T. M. Tran and Q. H. Nguyen, "Effect of blasting on the stability of lining during excavation of new tunnel near the existing tunnel," *Civ. Eng. J. Staveb. Obz.*, vol. 30, no. 1, pp. 47–62, 2021. https://doi.org/10.14311/cej.2021.01.0004

[12] R. S. Cheng, W. S. Chen, H. Hao, and J. D. Li, "A state-of-the-art review of road tunnel subjected to blast loads," *Tunn. Undergr. Space Technol.*, vol. 112, p. 103911, 2021. https://doi.org/10.1016/j.tust.2021.103911

[13] L. Z. Cheng, Z. Q. Yang, P. Zhao, and F. T. Li, "Damage characteristics of blasting surrounding rock in mountain tunnel in fault fracture zones based on the johnson-holmquist-2 model," *Buildings*, vol. 14, no. 11, p. 3682, 2024. https://doi.org/10.3390/buildings14113682

[14] R. L. Shan, Y. Zhao, H. L. Wang, Z. F. Liu, and H. F. Qin, "Blasting vibration response and safety control of mountain tunnel," *Bull. Eng. Geol. Environ.*, vol. 82, no. 5, p. 166, 2023. https://doi.org/10.1007/s10064-023-03199-z

[15] S. S. Bai, Z. Q. Zhou, C. L. Gao, T. Gao, G. H. Jin, and G. Z. Tao, "An FDM–DEM bridging domain coupling simulation method considering blasting dynamic disturbance for tunnel excavation," *Comp. Part. Mech.*, vol. 12, no. 5, pp. 3985–4001, 2025. https://doi.org/10.1007/s40571-025-01038-4

[16] W. M. Zhang, D. W. Liu, Y. Tang, W. C. Qiu, and R. P. Zhang, "Multifractal characteristics of smooth blasting overbreak in extra-long hard rock tunnel," *Fractal Fract.*, vol. 7, no. 12, p. 842, 2023. https://doi.org/10.3390/fractalfract7120842

[17] Y. Luo, H. L. Gong, D. X. Qu, X. P. Zhang, Y. H. Tao, and X. P. Li, "Vibration velocity and frequency characteristics of surrounding rock of adjacent tunnel under blasting excavation," *Sci. Rep.*, vol. 12, no. 1, p. 8453, 2022. https://doi.org/10.1038/s41598-022-12203-7

[18] M. Wang, W. J. Ding, D. K. Zhao, D. S. Liu, L. K. Wang, T. Zhang, and T. L. Ling, "Blasting vibration law and prediction in the near-field of tunnel," *Shock Vib.*, vol. 2022, pp. 1–11, 2022. https://doi.org/10.1155/2022/7412777

[19] X. Wang, J. C. Li, X. B. Zhao, and Y. Liang, "Propagation characteristics and prediction of blast-induced vibration on closely spaced rock tunnels," *Tunn. Undergr. Space Technol.*, vol. 123, p. 104416, 2022. https://doi.org/10.1016/j.tust.2022.104416

[20] Y. L. Wang, Z. S. Tan, and Y. L. Chi, "Research on blasting control technology for blast in shallow tunnel crossing existing buildings," *Appl. Mech. Mater.*, vol. 90, pp. 1768–1771, 2011. https://doi.org/10.4028/www.

scientific.net/AMM.90-93.1768

[21] J. Q. Zhao, H. Y. Ju, J. H. Li, and Y. P. Liu, "The monitoring technology research about the tunnel blasting vibration under the complex construction," *Adv. Mater. Res.*, vol. 594, pp. 1078–1081, 2012. https://doi.org/10.4028/www.scientific.net/AMR.594-597.1078

[22] J. J. Zhou, S. Gao, P. K. Luo, J. L. Fan, and C. C. Zhao, "Optimization of blasting parameters considering both vibration reduction and profile control: A case study in a mountain hard rock tunnel," *Buildings*, vol. 14, no. 5, p. 1421, 2024. https://doi.org/10.3390/buildings14051421

[23] X. D. Li, K. W. Liu, Y. Y. Sha, J. C. Yang, and Z. X. Hong, "Experimental and numerical investigation on rock fracturing in tunnel contour blasting under initial stress," *Int. J. Impact Eng.*, vol. 185, p. 104844, 2024. https://doi.org/10.1016/j.ijimpeng.2023.104844

[24] X. Li, Y. Long, C. Ji, M. Zhong, and H. Zhao, "Study on the vibration effect on operation subway induced by blasting of an adjacent cross tunnel and the reducing vibration techniques," *J. Vibroeng.*, vol. 15, no. 3, pp. 1454–1462, 2013.

[25] B. X. Jia, L. L. Zhou, J. J. Cui, and H. Chen, "Attenuation model of tunnel blast vibration velocity based on the influence of free surface," *Sci. Rep.*, vol. 11, no. 1, p. 21077, 2021. https://doi.org/10.1038/s41598-021-00640-9